

The Radial Velocity Variability of the K-giant γ Draconis: Stellar Variability Masquerading as a Planet

A. P. Hatzes

Thüringen Landessternwarte Tautenburg, Sternwarte 5, D-07778 Tautenburg, Germany

`artie@tls-tautenburg.de`

and

M. Endl

McDonald Observatory, The University of Texas at Austin, Austin, TX 78712, USA

and

W. D. Cochran

McDonald Observatory, The University of Texas at Austin, Austin, TX 78712, USA

and

P. J. MacQueen

McDonald Observatory, The University of Texas at Austin, Austin, TX 78712, USA

and

I. Han

*Korea Astronomy and Space Science Institute, 776 daedukdae-ro, Yuseong-gu, 305-348,
Taejeon, South Korea*

and

B.-C. Lee

*Korea Astronomy and Space Science Institute, 776 daedukdae-ro, Yuseong-gu, 305-348,
Taejeon, South Korea*

and

K.-M. Kim

*Korea Astronomy and Space Science Institute, 776 daedukdae-ro, Yuseong-gu, 305-348,
Taejeon, South Korea*

and

D. Mkrtichian

*National Astronomical Research Institute of Thailand, 191 Siriphanich Bldg., Huay Kaew
Rd., Suthap, Muang, 50200 Chiang Mai, Thailand*

*Astronomical Observatory, Odessa National University, Schechenko Park, Odessa, 65014,
Ukraine*

and

M. Döllinger

Thüringen Landessternwarte Tautenburg, Sternwarte 5, D-07778 Tautenburg, Germany

and

M. Hartmann

Thüringen Landessternwarte Tautenburg, Sternwarte 5, D-07778 Tautenburg, Germany

and

M. Karjalainen

*Isaac Newton Group of Telescopes, Apartado de Correos 321, Santa Cruz de la Palma,
E-38700, Spain*

and

S. Dreizler

*Institut für Astrophysik, Georg-August-Universität, Friedrich-Hund-Platz, 1, 37077,
Göttingen, Germany*

ABSTRACT

We present precise stellar radial velocity measurements of γ Dra taken from 2003 to 2017. The data from 2003 to 2011 show coherent, long-lived variations with a period of 702 d. These variations are consistent with the presence of a planetary companion having $m \sin i = 10.7 M_{\text{Jup}}$ whose orbital properties are typical for giant planets found around evolved stars. An analysis of the Hipparcos photometry, Ca II S-index measurements, and measurements of the spectral line shapes during this time show no variations with the radial velocity of the planet which seems to “confirm” the presence of the planet. However, radial velocity measurements taken 2011 – 2017 seem to refute this. From 2011 to 2013 the radial velocity variations virtually disappear only to return in 2014, but with a noticeable phase shift. The total radial velocity variations are consistent either with amplitude variations on timescales of ≈ 10.6 yr, or the beating effect between two periods of 666 d and 801 d. It seems unlikely that both these signals stem from a two-planet system. A simple dynamical analysis indicates that there is only a 1–2% chance that the two-planet is stable. Rather, we suggest that this multi-periodic behavior may represent a new form of stellar variability, possibly related to oscillatory convective modes. If such intrinsic stellar variability is common around K giant stars and is attributed to planetary companions, then the planet occurrence rate among these stars may be significantly lower than thought.

Subject headings: stars:variables:general — stars:oscillations — stars: individual (γ Dra) — stars: planetary systems — techniques: radial velocities

1. Introduction

Currently, G-K giants offer us one of the few means of studying the frequency of planets around intermediate mass (IM) stars ($1.3 - 3 M_{\odot}$) using the Doppler method. While on the main sequence an IM star is ill-suited for radial velocity (RV) measurements because it has few stellar lines that are often broadened by high rates of rotation. On the other hand, IM stars that have evolved onto the giant branch are cool, have lots of stellar lines and low rotation rates. A number of surveys have searched for exoplanets around giant stars with RV measurements (Setiawan et al. 2003; Döllinger et al. 2007; Johnson et al. 2007; Sato et al. 2008; Niedzielski et al. 2009; Wittenmyer et al. 2011; Jones et al. 2011; Lee et al. 2012).

Recently, Hrudková et al. (2017) started a program to search for exoplanets around K giant stars observed by the *Kepler* mission. This program exploits the fact that the stellar oscillations seen in the *Kepler* light curves can be used to derive accurate stellar masses.

Normally, one has to rely on theoretical evolutionary tracks and their inherent uncertainties. This program discovered the planet candidate around HD 175370. To date about 100 giant planets have been claimed around evolved G-K stars and most of these have orbital periods of several hundreds of days. Many of these are exoplanets whose nature has been confirmed. These include ι Dra b in an eccentric orbit (Frink et al. 2002) and more recently the transiting planet Kepler-91b (Barclay et al. 2015)

Because of the evolved status of K giant stars (i.e. extended atmospheres, deep convection zones, etc.) it should be a concern that these RV variations may actually arise from intrinsic stellar variability. Lately, there have been several planet candidates around K giants that can best be termed “problematical”. Ramm et al. (2009) discovered periodic variations in the K giant primary component of the binary system ν Oct. These had a period of 418 d and an amplitude of 50 m s^{-1} which were consistent with a planetary companion having a mass of a $2.4 M_{Jup}$. However, the orbital period of the binary system was only 1050 days which made the planet-binary system dynamically unstable. The stability of the system was only possible if the planet had a retrograde orbit with respect to the binary motion (Eberle & Cuntz 2010). More evidence supporting this hypothesis came from a lack of changes in the spectral line shapes as well as no observed line-depth variations, which were a measure of temperature variations, with the orbital period (Ramm 2015). It seems that the RV variations were not due to intrinsic stellar variability.

A recent study by Ramm et al. (2016) provided mixed results as to the reality of ν Oct Ab. Additional RV measurements for the star placed precise orbital and mass constraints on the retrograde planet, but these models were not stable for 10^6 years. However, the study did reveal a narrow range of parameter space where a few orbital models were stable for more than 10^8 years. Although the planet hypothesis seems less likely from a dynamical point of view, there is a small chance that the planet lies on a stable orbit.

There have been other “dynamically challenged” planets that have been found around other K giant stars. BD+20 2457 shows RV variations consistent with two planetary candidates with masses of $21.4 M_{Jup}$ and $12.5 M_{Jup}$ and periods of 380 d and 622 d, respectively (Niedzielski et al. 2009). No dynamically stable configuration was found for this system. Niedzielski et al. (2009) found RV variations in HD 102272 that were possibly due to two companions with masses of $5.9 M_{Jup}$ and $2.6 M_{Jup}$ orbiting in nearly a 4:1 resonance ($P = 127$ d and 520 d). However, a dynamical study showed that the planets would quickly collide with one another. Trifonov et al. (2014) found two giant planets in a 2:1 resonance around η Cet whose orbits was only stable for some configurations. The dynamical problems of all of these systems could be resolved if the RV variations of one of the purported planets were in fact due to stellar variability.

One star in the McDonald sample of K giant stars that was surveyed with RV measurements by Hatzes & Cochran (1993) from over two decades ago was γ Dra (= HR 6705 = HD 164058 = HIP 87833). RV measurements for this star showed long-term variability, but there was insufficient data to determine an accurate period. The RV monitoring of this star stopped in 1993, but re-started in 2003 in order to investigate further these long-term variations. These new measurements showed RV variations seem to be consistent with a planetary companion; however, additional measurements refute this hypothesis. γ Dra may be a case of stellar variability in a K giant which can mimic, for a time, the signal of a planet.

2. Stellar Parameters

The star γ Dra has a spectral type of K5 III and is located at a distance of 45 pc (van Leeuwen, 2007). Mozurkewich et al. (2003) measured an angular diameter of 9.86 ± 0.128 mas. For the distance of γ Dra this implies a stellar radius of $50.03 \pm 0.69 R_{\odot}$.

Several investigations have determined the stellar parameters. McWilliam (1990) measured an effective temperature of 3990 K, a surface gravity of $\log g = 1.55$, and an abundance that is slightly metal poor, $[Fe/H] = -0.14 \pm 0.16$. More recent measurements point to a higher metallicity for the star. Prugniel et al. (2011) found $[Fe/H] = +0.11 \pm 0.05$, $T_{\text{eff}} = 3990 \pm 60$ K, and $\log g = 1.64 \pm 0.1$. These values were consistent with those derived by Koleva & Vazdekis (2012): $[Fe/H] = +0.11 \pm 0.09$, $T_{\text{eff}} = 3990 \pm 42$ K, and $\log g = 1.669 \pm 0.1$.

The basic stellar parameters of mass, radius, and age were determined using the online tool from Girardi (<http://stev.oapd.inaf.it/cgi-bin/param>; version PARAM 1.3). This uses a library of theoretical isochrones (Girardi et al. 2000) and a modified version of the Jørgensen & Lindegren’s (2005) method. A detailed description of this method is given by da Silva et al. (2006).

The values of the calculated stellar parameters depend on the measured input parameters. Using the effective temperature and abundance of Koleva & Vazdekis (2012) results in $M = 2.14 \pm 0.16 M_{\odot}$, $R = 49.07 \pm 3.75 R_{\odot}$, and an age of 1.28 ± 0.29 Gyrs. The radius determined by this method, $R = 49.03 \pm 2.5 R_{\odot}$, is in excellent agreement with the interferometric value.

The luminosity of the star can be estimated using two approaches. With the first method we combine the stellar distance, apparent magnitude and bolometric correction to obtain the stellar luminosity. The absolute magnitude of γ Dra is -1.144 ± 0.015 . Buzzoni et al. (2010) give a bolometric correction of -0.99 ± 0.10 for $T_{\text{eff}} = 3990$ K. This yields a

total luminosity of $510 \pm 51 L_{\odot}$. Alternatively, one can use the measured stellar radius and effective temperature to calculate the total luminosity. For $T_{\text{eff}} = 3990$ K this yields $L = 515 \pm 37 L_{\odot}$. We simply adopt $510 L_{\odot}$ as the luminosity of γ Dra. Table 1 summarizes the stellar parameters.

3. The Data Sets

A total of four RV data sets were used in the analysis. These include observations made at the 2.1m and 2.7m telescopes at McDonald Observatory, the 1.8m telescope at the Bohunyanon Optical Astronomy Observatory (BOAO), and the 2m telescope at the Thüringer Landessternwarte Tautenburg (TLS). Table 2 lists the journal of observations including the time span of the measurements and the number of observations. Table 3 lists the RV measurements listed according to data sets.

3.1. The McD-2.1 Data Set

The earliest observations were made with the coude spectrograph of the 2.1m Otto Struve Telescope at McDonald Observatory. A 1200 grooves mm^{-1} grating was used in second order in combination with a Tektronix 512×512 CCD. Blocking filters were used to isolate the desired order. This instrumental setup resulted in a spectral dispersion of $0.046 \text{ \AA pixel}^{-1}$ at the central wavelength of 5520 \AA . An $85 \mu\text{m}$ slit provided a spectral resolution of 0.11 \AA (resolving power $R = \lambda/\Delta\lambda = 50\,000$). An iodine absorption cell placed in the light path of the spectrograph during the stellar observations provided the simultaneous wavelength calibration. See Hatzes & Cochran (1993) for more details of the instrumental setup and data reductions. Typically 2–10 observations were made of this star each night. These data are listed as “McD-2.1” in Table 3.

3.2. The McD-2.7 Data Set

The “McD-2.7” data set used the Tull Spectrograph (Tull et al. 1994) at the Harlan J. Smith 2.7m telescope. This instrument provided a nominal wavelength coverage of $3600 \text{ \AA} - 10\,000 \text{ \AA}$ at a resolving power of $R = 60\,000$. The RV measurement was extracted using self-calibrated I_2 spectra and the *Austral* RV-code (Endl, Kürster, & Els 2000).

3.3. The BOAO Data Set

RV measurements were also made with Bohyunsan Observatory Echelle Spectrograph or BOES (Kim et al. 2006) of the 1.8m telescope at the BOAO in South Korea. A 80 μm fiber resulted in a resolving power of $R = 90\,000$ with a wavelength coverage of 3600 – 10500 \AA . Relative RV measurements were made using an iodine absorption cell as a reference. These data are referred to as the “BOAO” set in Table 3.

3.4. The TLS Data Set

The TLS observations of γ Dra were made as part of the Tautenburg Observatory Planet Search (TOPS) program using the high-resolution coude echelle spectrometer of the Alfred Jensch 2m telescope and an iodine absorption cell placed in the optical path. The spectrometer is grism cross-dispersed and it has a resolving power $R = 67\,000$ and wavelength coverage 4630–7370 \AA . A more detailed description of radial velocity measurements from the TOPS program can be found in Hatzes et al. (2005). RV values are listed as “TLS” in Table 3.

4. Analysis of RV data

Figure 1 shows the RV measurements of γ Dra from the McD-2.7, BOAO, and TLS data sets. We will first focus our analysis on data taken from 2003 – 2011 which show a coherent, long-lived periodic signal, but only for the first half of the data. Afterwards we turn our analysis to using the full data set.

4.1. The 2003 – 2011 Data: Early evidence of a planetary companion

A periodogram analysis of the 2003 – 2013 RV data showed significant power at a frequency of $\nu = 0.00143\text{ d}^{-1}$ (period, $P = 699.3\text{ d}$) which is readily apparent in the time series. We fit a Keplerian orbit to these RV data using the program *Gaussfit* (Jefferys et al. 1988). Since each data set has its own zero-point velocity we allowed this to be a free parameter in the fitting process. Fortunately, there is good temporal overlap between the three data sets (TLS, McD-2.7, and BOAO). We note that all tabulated RV data are with the individual zero-points subtracted.

The derived orbital parameters are period, $P = 692.4 \pm 2.6\text{ d}$, radial velocity amplitude,

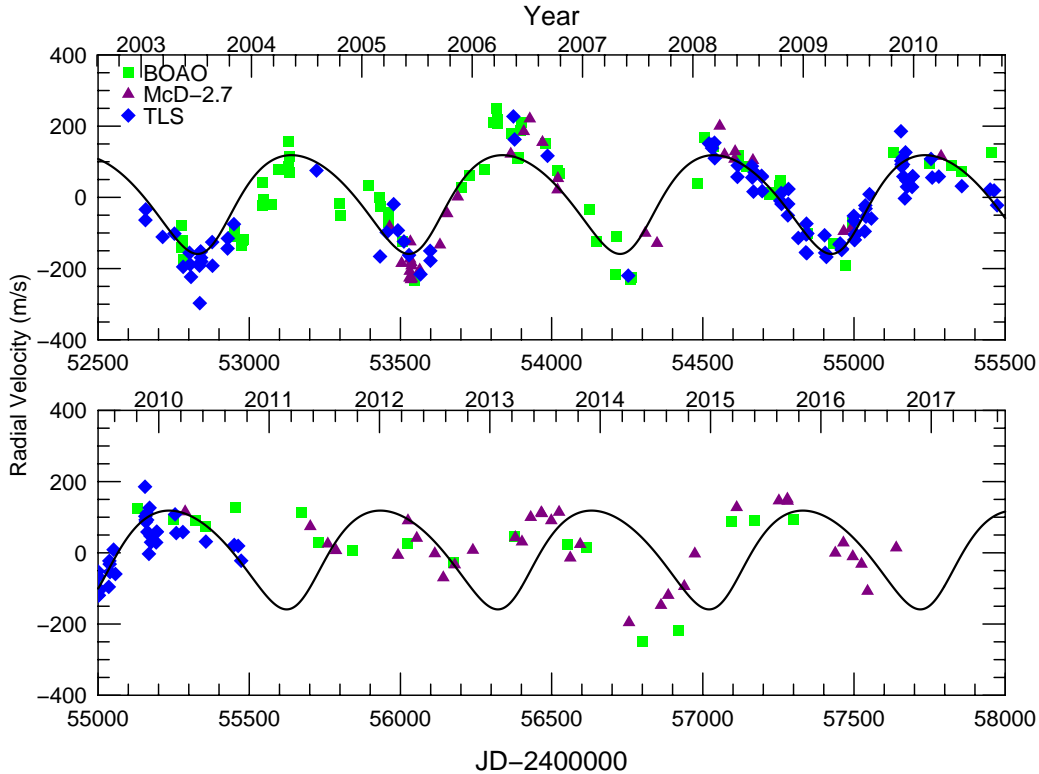


Fig. 1.— Radial velocity measurements for γ Dra from 2003 to 2017 taken with 3 different telescopes and instruments. Symbols: Triangles : McD-2.7, diamonds : TLS, squares : BOAO. The solid line represents the orbital solution (Table 4).

$K = 147.3 \pm 4.7 \text{ m s}^{-1}$, eccentricity, $e = 0.16 \pm 0.03$, time of periastron, $T_0 = 2446722.39 \pm 31.06$, and argument of periastron, $\omega = 203.7 \pm 13.5$ degrees.

The McD-2.1 RV measurements taken between 1991 and 1993 also show variations with a period of ~ 700 d (Fig. 2). When computing the Scargle periodogram (Scargle 1982) the power, z increases from $z \approx 74$ to $z \approx 83$ after adding the McD-2.1 data. This represents a decrease in the false alarm probability by a factor of $\approx 10^4$. The signal was apparently present in the earlier measurements, so we tried fitting a Keplerian orbit including these earlier measurements. This final orbit is shown by the line in Figs. 1 and 2. The parameters are listed in Table 4. The hypothetical companion has a minimum mass of $10.7 M_{Jup}$. Such a massive giant planet with a relatively long (few hundreds of days) orbital period is typical for planets around K giant stars.

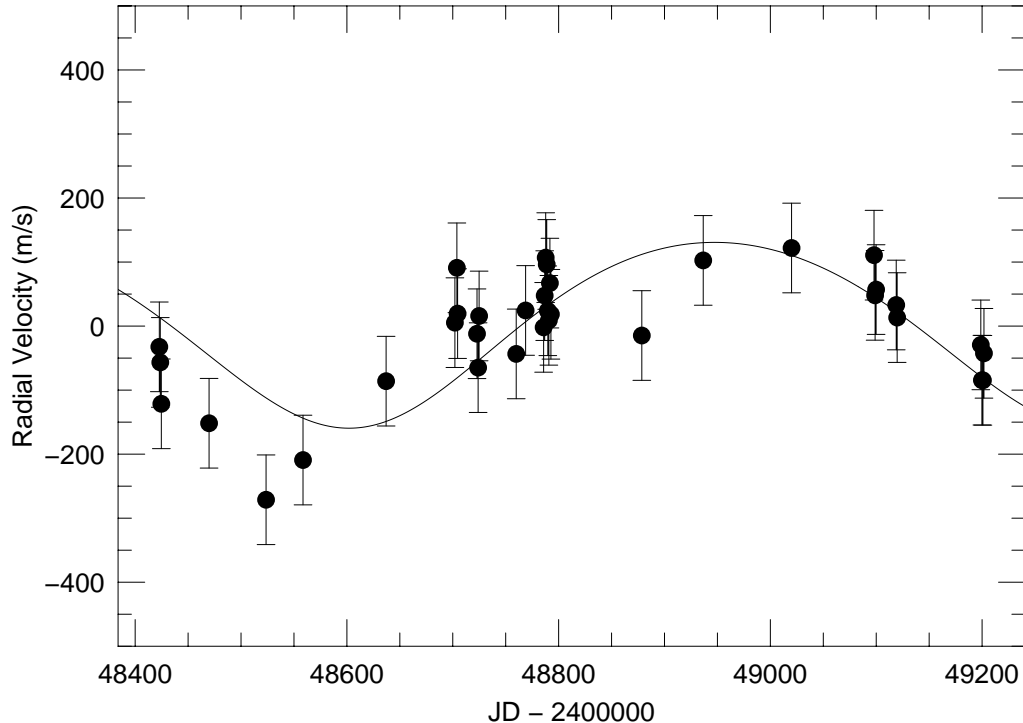


Fig. 2.— The McD-2.1 RV data (dots) and the orbital solution (line) using all the RV measurements taken up to 2011. The curve represents the orbital solution.

The top panel of Fig. 3 shows the RV variations phased to the orbital period. Even the earlier McD-2.1 data seem to follow the orbit reasonably well. The fourth column in Table 2 shows the rms scatter of the RV data sets about the orbital solution, but only for the time span 2003 – 2011. These have a mean error of $\approx 50 \text{ m s}^{-1}$, significantly larger than the internal measurement error, but entirely consistent with stellar oscillations. Using the scaling relationships of Kjeldson & Bedding (1995) we estimate a velocity amplitude for the pulsations, $v_{osc} \sim 55 \text{ m s}^{-1}$. The observed deviations of the RV from the orbital solution can thus be naturally explained by the intrinsic stellar jitter due to stellar oscillations.

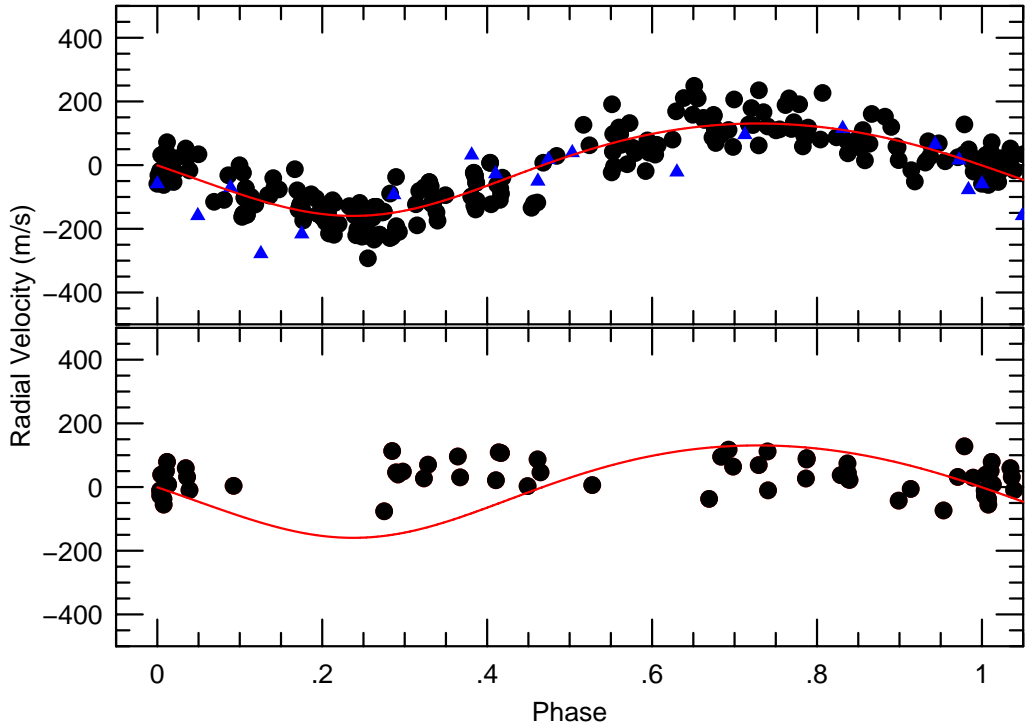


Fig. 3.— (Top) Radial velocity measurements for γ Dra taken 2003-2011 (dots) and phased to the orbital period of 702 d. The triangles represent the McD-2.1 data taken 20 years earlier. (Bottom) RV measurements taken 2011-2014 phased to the orbital period. The curve in both panels represent the orbital solution.

4.1.1. “Confirmation” of the purported planet

The RV measurements of γ Dra taken between 2003 and 2011 show strong evidence of orbital motion due to a planetary companion. However, as with all such “planet” discoveries we must exclude stellar variability (e.g. rotational modulation, pulsations, etc.) as a cause of the RV behavior. The examinations of the spectral line shapes, photometric variations and activity indicators have become common tools for the confirmation of planetary companions around stars, most notably K giant stars. It is of interest to see if these tools could have given us an indication that the RV variations of γ Dra were due to stellar variability. For this purpose we will examine only the time when the star showed clear periodic RV variations.

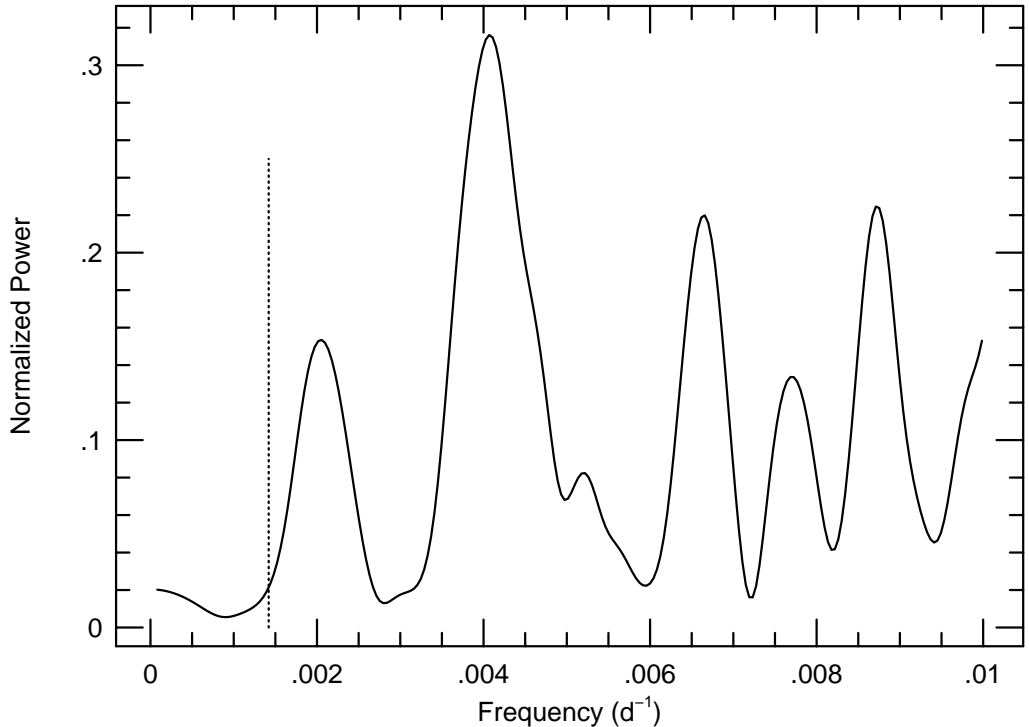


Fig. 4.— GLS periodogram of the Hipparcos photometry. The vertical line marks the location of the orbital frequency.

Hipparcos *Photometry*

It is difficult to get precise light curves on very bright stars like γ Dra using ground-based measurements. For discoveries from K giant planet search programs one generally has to rely on photometry taken by the Hipparcos space mission. This photometry is usually not contemporaneous with the RV data, but it is in the case for the early McD-2.1 measurements. The Generalized Lomb-Scargle (GLS) periodogram (Zechmeister & Kürster 2008) of the Hipparcos photometry shows no significant power at the orbital frequency (Figure 4). The rms scatter of the photometric measurements is only about 4.8 millimag.

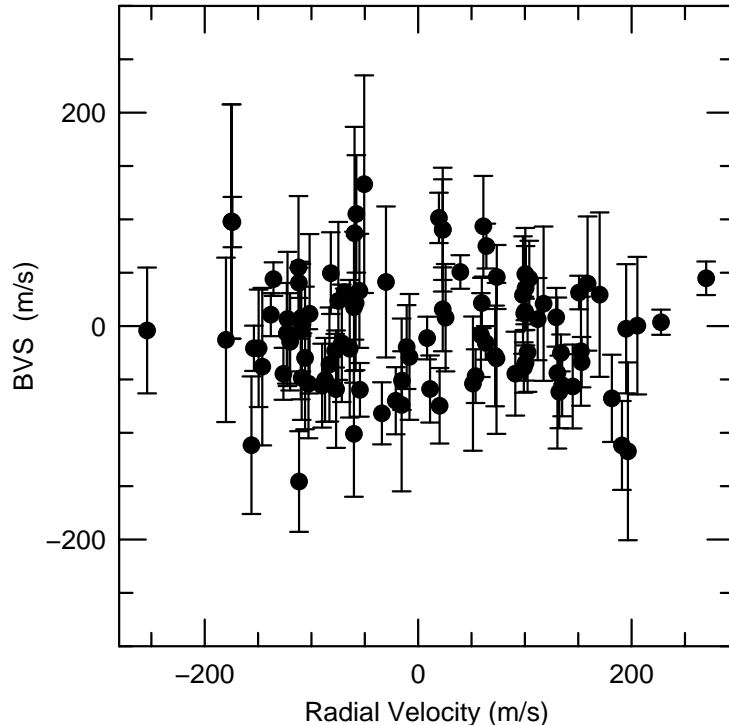


Fig. 5.— The bisector velocity span (BVS) versus the RV

Line Bisector Variations

Another means of testing for the planetary nature is to search for variations in the shapes of the spectral lines with the spectral line bisector (Hatzes, Cochran, & Johns-Krull 1997; Hatzes, Cochran, & Bakker 1998; Queloz et al. 2001). Whereas pulsations or stellar surface structure should produce RV variations that are accompanied by line shape variations, the orbital motion due to a companion will cause an overall Doppler shift of the spectral line without any changes in the line shape.

To investigate any changes in the spectral line shapes we first calculated the cross-correlation function (CCF) using one of our observations as a template, but restricting the calculation to the spectral region 4720–4900 Å which is largely free of iodine absorption lines. Only the TLS data was utilized for several reasons. First, the TLS echelle spectrograph has few moving parts. One only has to move different gratings that are mounted on a slide into the light path in order to access a different wavelength region. The spectrograph is typically

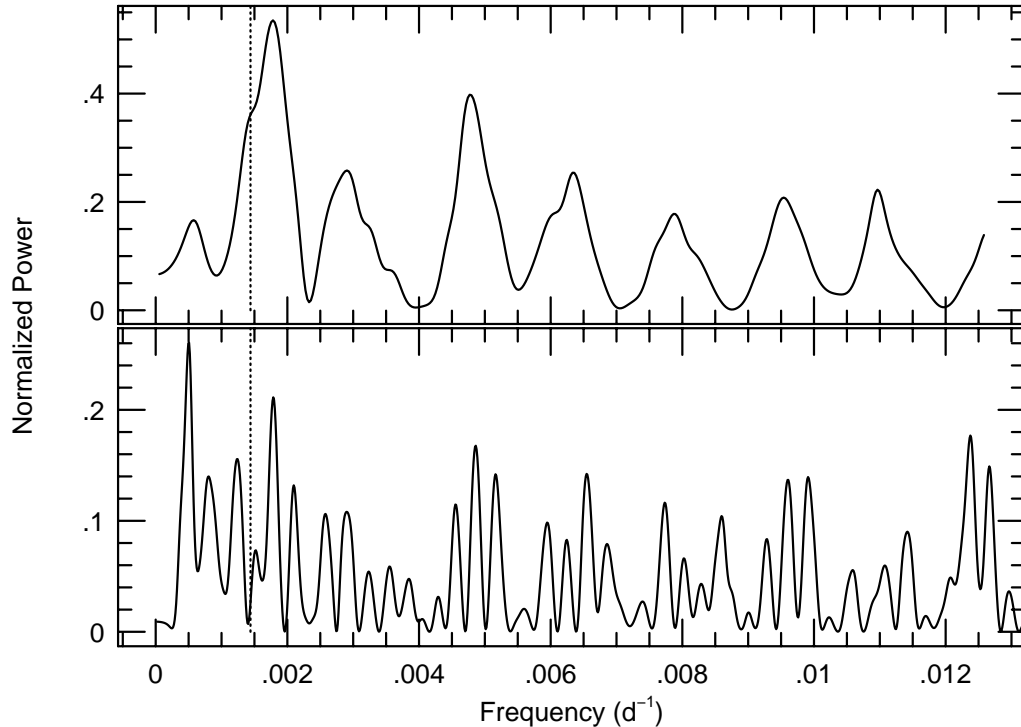


Fig. 6.— (top) GLS periodogram of the Ca II SMCd-index during 2003 - 2011. (bottom) GLS periodogram of the SMCd-index for the full data set. The vertical dashed line marks the orbital frequency of the purported planet.

used in the exact same setup over a time span of several months. This ensures a relatively stable instrumental profile (IP) which is important since in measuring the shape of the CCF we are not taking into account any possible change in the IP. Second, in looking for line shape variations it is important to have as high a spectral resolution as possible. The TLS data has slightly higher resolving power over the McD-2.7 data. The BOAO data have higher spectral resolution, but the IP is more unstable compared to the TLS data (Han et al. 2010). The RV calculation takes into account changes in the IP, but not so for the bisector measurements.

We calculated the bisector of the CCF – the locus of the midpoints calculated from both sides of the CCF having the same relative flux value. A linear least-squares fit was then made to the CCF bisectors. We then converted this slope between the CCF height values of 0.3 and 0.85 to an equivalent velocity which we will call the bisector velocity span

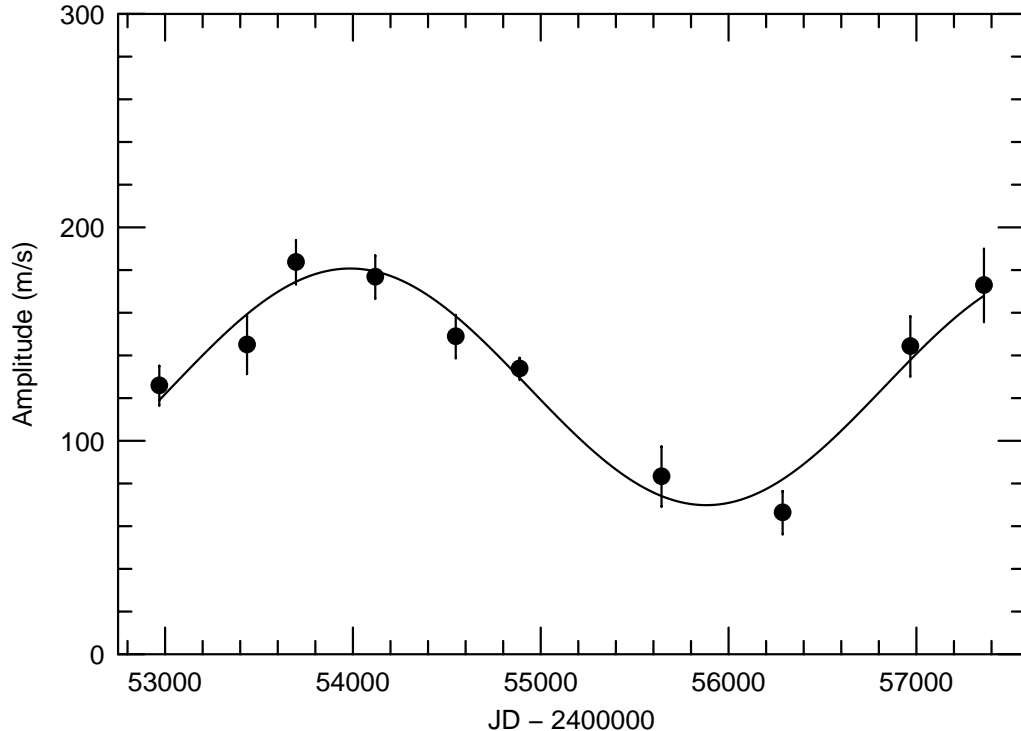


Fig. 7.— Amplitude variations of the 702-d period found in the RV measurements. The curve represents a sine-fit with a period of 10.6 years

(BVS). Figure 5 shows the correlation of the BVS with the RV measurements. There is no clear correlation between the two quantities as the probability that they are uncorrelated is 0.48. The 702-d RV variations do not seem to be accompanied by line shape variations. Note that there is a large range in the RV variations not seen in the BVS.

Ca II Variations and Rotational Modulation

The wavelength coverage of the McD-2.7m data includes the Ca II K line. In the past a “McDonald S-index” has been used to search for chromospheric variability in stars that are candidates to host extrasolar planets (e.g. Hatzes et al. 2015). The mean McDonald S-index, SMcD-index, should not to be confused with the Mt. Wilson S-index (see Paulson et al. 2002 for a definition of the SMcD-index). Normally, we can use the mean SMcD-index as a measure of the activity level of the star, but this is not the case for a giant star such

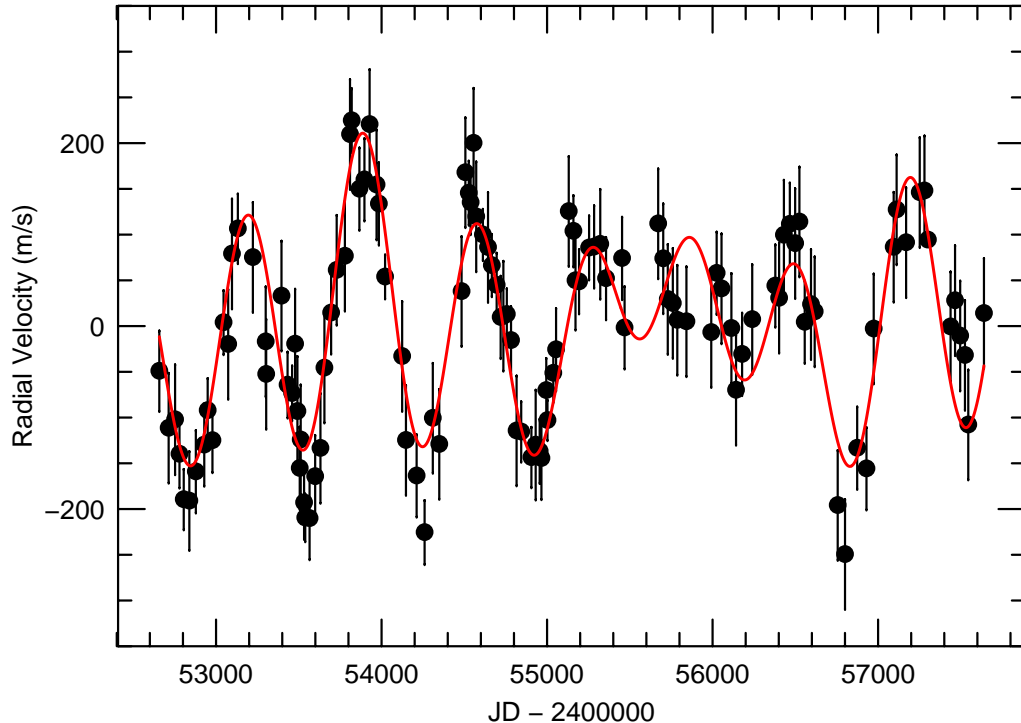


Fig. 8.— Three component sine-fit (curve) to the RV data from 2003-2017 using the parameters found in the pre-whitening process (Table 5). The error bars represent the rms scatter about the solution.

as γ Dra due to calibration issues between giants and dwarfs. However, we are not so much interested in the mean activity level of γ Dra, but whether chromospheric variability might be related to the RV variations. For our purposes the relative changes in the SMcD-index is what is important.

The top panel of Fig. 6 shows the GLS of the Ca II SMcD-index during 2003 – 2011, the time when the 702-d variations were present in the RV measurements of γ Dra. The highest peak occurs at a period of 560 d (frequency = 0.00178 d^{-1}), GLS yields a nominal false alarm probability (FAP) of $\approx 1 \%$ for the peak. However, a bootstrap analysis by randomly shuffling the time stamps of the data and examining the resulting periodograms yielded a much higher FAP $\approx 10 \%$. The peak is marginally significant, but if it is a real signal it is clearly displaced from the orbital frequency. The power of this peak weakens when analyzing the full data set, but is still present (lower panel of Fig. 6). If real, we believe that this period

corresponds to the rotational period of the star.

We can estimate the rotational period, P_{rot} , of the star from the stellar radius and projected rotational velocity, $v \sin i$. Massarotti et al. (2008) measured a $v \sin i = 6 \text{ km s}^{-1}$ for γ Dra. Combined with the interferometric radius of the star yields $P_{rot} \approx 400 \text{ d}$. This $v \sin i$ determination may be somewhat high. We also estimated the projected rotational velocity using our high-resolution spectra. We fit a few selected spectral lines with synthetic line profiles that were broadened by macroturbulence and rotation. For the macroturbulence we use a value of 6 km s^{-1} which is typical for giant stars with the same surface gravity and temperature of γ Dra (Carney et al. 2008). A good fit to the spectral lines was obtained for $v \sin i \approx 4 \pm 1 \text{ km s}^{-1}$. This yields a rotational period of $600 \pm 150 \text{ d}$. So, our best guess for the rotational period of γ Dra is 400-600 d. This is consistent with the 560-d period found in the subset SMcD-index measurements. We take this as the nominal rotational period of the star.

We caution the reader, however, that this estimate of the rotational period is uncertain. The peak SMcD-index periodogram is not convincingly significant. The estimated rotational period also depends on the measured $v \sin i$ which is difficult to determine accurately for slowly rotating stars. Differential rotation, which may be significant in K giant stars, only complicates matters.

The RV data taken up until 2011 show variations long-lived, and coherent for at least 7 years and arguably 20 years when including the measurements from the 2.1-McD data set. The standard tools of planet confirmation - lack of photometric and line profile variations - also support the planet hypothesis. Had we stopped our RV measurements in 2011, a logical conclusion would be that the RV variations seen in γ Dra arise from the presence of a signal planetary companion.

It is clear from the lower panel of Figure 1 that starting in 2011 the characteristics of the RV variations abruptly changed. Between 2011 and 2014 the RV was relatively constant, or at least there was no evidence for strong periodic variations. Starting near 2014 the periodic variations returned with the same amplitude, but with a clear phase shift of about 0.20. Thus, the RV data from 2011 onward appear to refute the planetary hypothesis.

4.2. Amplitude Variations

The RV measurements of γ Dra show a hint of amplitude variations in the 2003-2011 data. For instance, the RV seems to be systematically higher than the orbital solution during 2006–2007. To investigate possible amplitude variations we divided the RV variations into

slightly overlapping time segments. For each time subset we fit a sine wave to the data keeping the period fixed to 702 d, but allowing both the amplitude and phase to vary. Fitting these amplitudes with a sine function results in a period of $P = 3793 \pm 108$ d (Fig. 7).

4.3. Frequency analysis of the full data set

The beating of two closely-spaced periods can also mimic amplitude variations and these periods should be evident in a Fourier analysis of the full data set. We performed a frequency analysis using the program *Period04* (Lenz & Breger 2005). A pre-whitening approach was used, i.e. the dominant period in the data was found, a sine-function fit to this and the signal was subtracted. We then searched the residual RVs and found three significant signals (FAP < 0.01) in the RV data and these are listed in Table 5. To assess the FAP we use the criterion that a peak having an amplitude at least four times higher than the surrounding noise level has a FAP ≈ 0.01 (Kuschnig et al. 1997). The phase is reckoned starting at JD = 2452656.6641. Two of these, $P_1 = 665.8$ d and $P_2 = 800.9$ d will produce beat-related amplitude variations of 3945 d, very close to the period of the observed amplitude variations. The fit to the RV data using the three sine components is shown in Figure 8. The rms scatter about this fit is 49 ms^{-1} . The error bars represent this scatter which is a more realistic estimate of the RV error that includes intrinsic stellar variability (the so-called “jitter”).

5. The Nature of the Multi-periodic Signals

The observed amplitude variations can be explained by the presence of two signals, P_1 and P_2 with closely-spaced in period. Two possible hypotheses for these are 1) a two-planet system or 2) stellar oscillations.

5.1. A Two-planet System

We can denote the semi-major axis of the outer planet by $a = 1 + \Delta$, where Δ is the fractional separation, and μ_1 and μ_2 the mass ratios of the two planets with respect to the host star. The velocity K-amplitude of P_1 and P_2 imply companion masses of $\approx 9 M_{Jup}$ and $3.5 M_{Jup}$, respectively. The orbits are stable if $\Delta > 2.4(\mu_1 + \mu_2)^{1/3}$ (Gladman 1993). For γ Dra $2.4(\mu_1 + \mu_2)^{1/3} = 0.56$, much larger than the value of $\Delta = 0.12$. At first glance the system seems unstable.

A proper assessment of the stability of the system can only come from numerical simulations. Possibly there are some configurations for which the system would be stable. To do this we started from a Keplerian model restricted to circular orbits (see Table 5). The best-fit Keplerian solution of a two-planet system is very unfavorable for a dynamically stable configuration. The rather large planetary masses, the small difference in semi-major axes and the absence of a mean motion resonance make it unlikely to find long-term stable configurations. In order to estimate the fraction of stable configurations, we used the N-body integrator *Mercury6* (Chambers 1999) to investigate the dynamical stability.

In a first step, co-planar configurations with $i = 90^\circ$ were investigated using 1000 random variations of the start parameters (mass, mean anomaly, and semi-major axis) within the estimated uncertainties. The mass of the central star was kept fixed at $2.14 M_\odot$. In our calculations, 28 out of the 1000 configurations survived more than 1 Myr, however, most of the configurations were dynamically unstable on time scales of few orbits. Given the small difference of the semi-major axes this is not surprising. Since not all of the configurations were unstable on short time scales, we also allowed for mutual inclinations in a second run in order to search in a larger parameter space. Out of 30000 randomly chosen start configurations 514 survived 1 Myr. This is a lower fraction of stable configurations. While the mutual inclinations help to avoid close encounters, the increasing mass at lower inclinations of the planets increases the gravitational interaction which counterbalances the former effect. For four of these we tested the dynamical stability over the estimated age of the star (1.6 Gyr). Two out of the four also survived.

Although this is a coarse investigation of the dynamical properties of a potential two-planet configuration, we nevertheless cannot outright exclude that a two-planet system is indeed stable. The probability for this is low at about 1-2%. Given such a low probability, a more detailed dynamical investigation is required, but that is beyond the scope of this paper.

5.2. Stellar Oscillations?

The RV variability of γ Dra may be related to the Long Period Variables (LPV). These stars pulsate with periods much longer than the fundamental radial mode. LPVs include, among others M giant stars, Mira variables as well as semi-periodic variable stars (SPV). Hinkle et al. (2002) investigated the velocity variability of a sample of nine LPVs and found that six showed periodic variations with periods, $P = 300 - 900$ d and amplitudes of ≈ 2 km s $^{-1}$. They proposed that these were a new form of stellar oscillations.

As an example, we take one star from their sample, g Her, that had good stellar parameters as listed in the *Simbad* database. The RV variations had $P = 843$ d with a K-amplitude of 2.3 km s^{-1} . We estimate that g Her has a luminosity of $L = 7300 L_{\odot}$ or about 14 times the luminosity of γ Dra. For the sake of argument, let us assume that the “pulsations” are related to high degree p-mode oscillations so that we can apply the scaling relationships of Kjeldsen & Bedding (1995). These indicate that the velocity amplitude of the oscillations, v_{osc} , scales as $v_{osc} \propto L$. Scaling from the g Her oscillations we thus expect $v_{osc} \sim 135 \text{ m s}^{-1}$ for γ Dra, comparable to the observed RV amplitude.

The photometric amplitude can also be estimated from the scaling relationships: $\delta L/L \propto v_{osc}$. Kiss et al. (1999) measured a photometric amplitude of ~ 0.2 mag for this period. This implies a photometric amplitude of ~ 0.02 for γ Dra. This is comparable to the peak-to-peak variations in the Hipparcos photometry (~ 0.01 mag), although this shows no periodic variability. However, given the uncertainties in estimating photometric variations, it is possible that these have an amplitude lower than the Hipparcos detection limit.

However, it is unlikely that the hypothetical oscillations in γ Dra are p-mode oscillations. A more likely hypothesis is that they may be related to dipole oscillatory convection modes in red giants. Saio et al. (2015) proposed these as a possible explanation of the long secondary period in LPVs. Oscillatory convective modes are non-adiabatic g^{-} modes that are present in luminous red giant stars with luminosities $\log(L/L_{\odot}) \gtrsim 3$.

The Period-Luminosity (P-L) for radial pulsators lie on roughly a straight line in the $\log(L)$ - $\log(P)$ plane. In contrast, the P-L relations of oscillatory convective modes have a peculiar shape that bends and becomes more horizontal for less luminous stars. Figure 9 shows a sample model from Saio et al. (2015) for stars with three different stellar masses (1.0, 1.3, and $2.0 M_{\odot}$) and a mixing length, $\alpha = 1.2$. The diagonal line shows a “by eye” fit to the LPV of the so-called “D” branch found by Soszynski et al. (2009). The location of γ Dra seems to be consistent with the $1.3 M_{\odot}$ model if one extrapolates this to lower luminosities. This model has a higher mass than our inferred mass for γ Dra, but given the uncertainties in this first calculation (convection, metallicity, etc.) the hypothesis that we are seeing oscillatory convective modes in γ Dra seems at least plausible.

6. Discussion

The long-term RV monitoring of γ Dra shows ostensibly the “rise and fall” of an exoplanet. The “rise” occurs over seven years (2003 – 2011). This is characterized by apparently stable, coherent variations with a period of 702 d that are consistent with a planetary

companion having a minimum mass of $10.7 M_{Jup}$. This “planetary companion” has characteristics that seem typical for giant planets around K giant stars - massive planets with orbital periods of several hundreds of days. An examination of the bisector velocity span and photometric measurements from Hipparcos revealed no variations with the RV period. The case for the planet hypothesis is more credible by the fact that the RV variations of this planet seems to have been present in data taken 20 years earlier. Furthermore, our best estimate of rotational period for the star (560 d) derived from the Ca II data suggests, at face value, that the 702-d period is not the rotational period of the star.

The RV measurements taken from 2014–2016, however, contradict this conclusions and thus mark the “fall” of the planet candidate. The periodic RV variations abruptly cease and appear to be absent for the ensuing 3 years. They suddenly appear in 2016 with the same K -amplitude and period, but with a clear phase shift of approximately 0.2. It is difficult to reconcile these variations with the planet hypothesis.

There are two explanations for the amplitude variations. One, these may be due to a single period whose amplitude is changing with a period of approximately 10.6 yr. This also would have to be accompanied by phase shift in 2007. A plausible mechanism for this would be the decay of an active region that completely disappears by 2011 followed by the emergence of a new one, at a different location of the star starting in mid-2013. If true, it is puzzling why we do not see any evidence for this in the standard activity indicators. However, we know very little about the nature of any possible surface activity on giant stars and maybe these are not accompanied by measurable changes in the photometry, line bisectors, or Ca II emission.

Alternatively, the amplitude variations can simply arise from the beating of two closely-spaced periods, $P_1 = 666$ d and $P_2 = 801$ d. This is the simplest and most likely explanation. Furthermore, it appears to provide a natural explanation for the phase shift seen in 2014 (Fig. 8). We can only speculate as to the nature of these periods.

We cannot completely rule out that these two periods arise from a two-planet system. However, such a system would qualify as another “dynamically challenged” K-giant system. Our simple dynamical analysis suggests that there is only about 1–2 % chance that the orbits of the two-planet system are stable. One could argue that it is an unlikely system, but we see the system, so nature has found a way to produce it. Unfortunately, we cannot conclusively refute the 2-planet hypothesis.

On the other hand, one could argue that either P_1 or P_2 is due to a planetary companion, and that the other is due to rotational modulation of surface features. The 666-d period can be consistent with the generous estimate of the rotational period of 400–600 d. Again,

the rotational modulation in the RV would have to produce no variations in other quantities (bisector, Ca II, photometry). Although we cannot exclude this hypothesis, we do not favor it for the simple reason that whenever a beat phenomena between two closely oscillations is a prime suspect. At the present time we favor stellar oscillations as the cause of P_1 and P_2 .

The frequency analysis of the full data set reveals yet a third period, P_3 , at 1855 d which is significant. We cannot exclude that this signal is in fact due to a planetary companion with a minimum mass of $2.8 M_{Jup}$. However, given the fact that we have found two other long periods that are most likely due to stellar oscillations, it would be premature at this time to attribute a third long period to a companion. Continued monitoring of the star should be able to verify this.

Hatzes et al. (2015) reported two periods (629 d and 520 d) in the RV measurements of the K giant star α Tau that spanned 30 years. The longer period was attributed to the presence of a planetary companion while the 520-d period was interpreted as rotational modulation. Given that the periods found in α Tau are comparable to those in γ Dra and both stars are evolved with large radii, a closer scrutiny of the RV variability of α Tau is warranted.

The RV variations that we have discovered in γ Dra are both troubling and exciting. The troubling aspect stems from the fact that seven years of RV measurements for this star showed clear periodic variations that were long-lived and coherent. An orbital fit yielded a period and companion mass that was typical for planets around K giant stars. The scatter about the orbital fit could easily be explained by short-term oscillations on time scales of days and night-to-night variations of 50 m s^{-1} or more (see Table 3). An examination of the Hipparcos photometry and line bisectors showed no variations with the planet period. The standard tools used to confirm planet discoveries seem to have failed in this case.

One can only speculate as to how many of the giant planets around K giant stars may actually be due to stellar variability like the one we have found for γ Dra. Can this new phenomenon explain some of the “problem” multi-planets around K giant stars? Are there other instances where this new-found stellar variability is masquerading as a planet? In the case of γ Dra using seven years of observations we would have arrived at a logical conclusion (planetary companion) that may be wrong. Only after long-term monitoring (\sim decade) did the star reveal a more complicated nature for these variations.

The exciting aspect of our RV measurements is that we may have stumbled upon a new phenomenon in K giant stars, and quite possibly a new type of stellar oscillations. More studies are needed to investigate the nature of these RV variations. In particular, how these correlate with the evolutionary status of the star. Interestingly, γ Dra is highly evolved and

with a large radius. Perhaps this holds the key to understanding these variations. When looking for exoplanets around giant stars with the RV method, long-term monitoring over many years is required. Our observations of γ Dra only highlights that the community should be more critical in examining the nature of long-period RV variations in K giants and to not be so eager to attribute these to exoplanets.

This research has made use of the SIMBAD data base operated at CDS, Strasbourg, France. APH acknowledges the support of DFG grants HA 3279/5-1 and HA 3279/8-1. The McDonald Observatory Planet Search (ME, WDC, PJM) is supported by the National Science Foundation through grant AST-1313075.

REFERENCES

- Barclay, T., Endl, M., Huber, D. et al. 2014, *ApJ*, 800, 46
- Buzzoni, A., Patelli, L., Bellazzini, M., Pecci, F., Fusi, O.E. 2010, *MNRAS*, 403, 1592
- Carney, B.W., Gray, D.F., Yong, D., Latham D.W., Manset, N., Zelman, R., & Laird, J. 2008, *AJ*, 135, 892
- Chambers, J.E. 1999, in *Impact of Modern Dynamics in Astronomy, Colloquium 172 of the International Astronomical Union, Namur (Belgium) 6-11 July 1998*, p. 449
- da Silva, L., Girardi, L., Pasquini, et al. 2006, *A&A*, 458, 609
- Döllinger, M.P., Hatzes, A.P., Pasquini, L. et al. 2007, *A&A*, 472, 649
- Eberle, J., Cuntz, M. 2010, *A&A*, 514, 19
- Endl, M., Kürster, M., & Els, S. 2000, *A&A*, 362, 585
- Frink, S., Mitchell, D.S., Quirrenbach, A. et al. *ApJ*, 576, 478
- Girardi, L., Bressan. A., Bertelli, G., Chiosi, C. 2000, *A&AS*, 141, 371
- Gladman, B. 1993, *Icarus*, 106, 247
- Han, I., Lee, B.-C., Kim, K.M., Mkrtichian et al. 2010, *A&A*, 509, A24
- Hatzes, A. P. & Cochran, W. D. 1993, *ApJ*, 413, 339
- Hatzes, A.P., Cochran, W.D., Johns-Krull, C.M. 1997, *ApJ*, 478, 374

- Hatzes, A.P., Cochran, W.D., Bakker, E.J. 1998, *Nature*, 391, 154
- Hatzes, A. P., Guenther, E. W., Endl. M. et al. 2005, *A&A* 437, 743
- Hatzes, A. P., Cochran, W. D., Endl, M. et al. 2015, *A&A*, 580, 31
- Hinkle, K.H., Lebzelter, T., Joyce, R.R., Fekel, F.C. 2002, *AJ*, 123, 1002
- Hrudková, M, Hatzes, A., Karjalainen, R. et al. 2017, *MNRAS*, 464, 1018
- Jefferys, W., Fitzpatrick, J., McArthur, B. 1988, *Celest. Mech.* 41, 39.
- Johnson, J.A., Fischer, D.A., Marcy, G.W. et al. 2007, *ApJ*, 665, 785
- Jones, M. I., Jenkins, J.S., Rojo, P., Melo, C.H.F. 2011, *A&A*, 536, 71
- Jørgensen, and B.R., Lindegren, L. 2005, *A&A*, 436, 127
- Kim, K. M., Mkrtichian, D. E., B.-C. Lee, Han, I., & Hatzes, A. P. 2006, *A&A*, 454, 8
- Kiss, L.L., Szatmáry, K., Cadmus, R.R., Jr., Mattei, J.A. 1999, *A&A*, 346, 542
- Kjeldsen, H. & Bedding, T.R. 1995, *A&A*, 87, 106
- Koleva, M., Vazdekis, A. 2012, *A&A*, 538, 143
- Kuschnig, R., Weiss, W.W., Gruber, R., Bely, P.Y., Jenkner, H. 1997. *A&A*, 328, 544
- Kjeldsen, H. & Bedding, T.R. 1995, *A&A*, 87, 106
- Lee, B.-C., Mkrtichian. D. E., Han, I., Park, M.-G., Kim, K.-M. *A&A*, 548, 118
- Lenz, P., Breger, M., 2005, *CoAst*, 146, 53
- Massarotti, A., Latham, D., Stefanik, R.P., & Fogel, J. 2008, *AJ*, 135, 209
- McWilliam, A. 1990, *ApJS*, 74, 1075
- Mozurkewich, D., Armstrong, J. T., Hindsley, R.B. et al. 2003, *AJ*, 126, 2502
- Niedzielski, A., Goździewski, Wolszczan, A. et al. 2009 *ApJ*, 693 276
- Paulson, D. B., Saar, S. H., Cochran, W. D., & Hatzes, A. P. 2002, *AJ*, 124, 572
- Prugniel, Ph., Vauglin, I., Koleva, M. *A&A*, 531, 165
- Ramm, D.J. 2015, *MNRAS*, 449, 4428

- Ramm, D.J., Pourbaix, D., Hearnshaw, J.B., Komonjinda, S. 2009, MNRAS, 394, 1695
- Ramm, D.J., Nelson, B.E., Endl, M. et al. 2016, MNRAS, 460, 3706
- Queloz, D., Henry, G. W., Sivan, J. P. et al. 2001, A&A, 379, 279
- Saio, H, Wood, P.R., Takayama, M., Ita, Y. 2015, MNRAS, 452, 3863
- Sato, B., Izumiura, H., Toyota, E. et al. 2008, PASJ, 60, 539
- Scargle, J.D. 1982, ApJ, 263, 835
- Setiawan J. Hatzes, A.P., von der Lühe, O. et a. 2003, A&A, 398, 19
- Soszynski, I., Udalski, A., Szymanski, M.K. et al. 2009, AcA, 59. 335
- Trifonov, T., Reffert. S., Tan, X. et al. 2014, A&A, 568, 64
- Tull, R.G., MacQueen, P.J., Sneden, C., & Lambert, D.L. 1995, PASP, 107, 251.
- van Leeuwen, F. 2007, A&A, 474, 653
- Wittenmyer, R.A., Endl, M., Wang, L. et al. 2001, ApJ, 743, 184
- Zechmeister, M., Kürster, M. 2008, A&A, 491, 531

Parameter	Value
T_{eff} [K]	$3990 \pm 42 \text{ K}^1$
$\log g$	1.67 ± 0.1^1
[Fe/H]	$+0.11 \pm 0.05^1$
$v \sin i$ [km s^{-1}]	4.5 ± 0.05
Mass [M_{\odot}]	$2.14 \pm 0.16 M_{\odot}$
Angular Diameter [mas]	9.86 ± 0.128
Parallax [mas]	21.14 ± 0.10
Radius [R_{\odot}]	$49.03 \pm 2.52 R_{\odot}$
Age	$1.30 \pm 0.25 \text{ Gyr}$
V -mag	2.23 ± 0.009
$B - V$	1.52
L [L_{\odot}]	510 ± 51

Table 1: Stellar Parameters for γ Dra (¹Koleva & Vazdekis (2012), ²Mozurkewich et al. (2003)).

Data Set	Coverage (Years)	N	σ_{RV} (m s^{-1})
McD-2.1	1991.45–1993.58	35	64.1
McD-2.7	2005.26–2016.69	65	41.3
BOAO	2003.38–2015.76	82	57.5
TLS	2003.04–2013.57	136	47.1

Table 2: The data sets used in the orbital solution.

Julian Day	RV (m s^{-1})	σ (m s^{-1})	Dataset
2448422.8047	-30.13	10.6	McD-2.1
2448423.7305	-53.03	6.6	McD-2.1
2448424.7188	-114.12	7.0	McD-2.1
2448469.8125	-156.97	5.5	McD-2.1
2448523.6406	-270.98	12.4	McD-2.1
2448558.5547	-227.34	9.9	McD-2.1
2448637.0312	-88.92	19.8	McD-2.1
2448702.0156	3.13	28.1	McD-2.1
2448703.9336	68.52	19.8	McD-2.1
2448704.8594	8.29	14.6	McD-2.1
2448722.9062	-11.24	14.0	McD-2.1
2448723.9492	-59.35	21.2	McD-2.1
2448724.9023	9.06	10.7	McD-2.1
2448759.9336	-32.54	4.7	McD-2.1
2448768.8125	29.69	15.0	McD-2.1
2448785.8242	-2.20	10.2	McD-2.1
2448786.8398	51.03	8.9	McD-2.1
2448787.7891	108.23	5.5	McD-2.1
2448788.7539	96.43	7.8	McD-2.1
2448789.7852	24.33	4.4	McD-2.1
2448790.7773	6.89	7.2	McD-2.1
2448791.7656	70.90	5.7	McD-2.1
2448792.7188	18.73	6.3	McD-2.1
2448878.5820	-14.54	6.9	McD-2.1
2448936.5859	96.78	17.7	McD-2.1
2449020.0312	134.83	15.0	McD-2.1
2449097.9180	109.35	6.2	McD-2.1
2449098.9375	48.95	7.5	McD-2.1
2449099.8906	61.57	4.4	McD-2.1
2449118.8867	44.23	8.2	McD-2.1
2449119.7773	-0.99	6.7	McD-2.1
2449198.8008	-31.88	5.3	McD-2.1

Table 3: The RV Data

Julian Day	RV (m s^{-1})	σ (m s^{-1})	Dataset
2449199.8086	-91.47	12.4	McD-2.1
2449200.7930	-93.08	10.5	McD-2.1
2449201.7617	-56.20	9.8	McD-2.1
2453463.9492	-82.24	4.23	McD-2.7m
2453503.9023	-185.06	6.03	McD-2.7m
2453529.9492	-226.13	2.83	McD-2.7m
2453530.9296	-207.21	2.81	McD-2.7m
2453531.7968	-172.82	2.86	McD-2.7m
2453532.8593	-124.47	3.61	McD-2.7m
2453533.8476	-225.33	2.86	McD-2.7m
2453534.8320	-230.59	2.62	McD-2.7m
2453535.8320	-182.47	2.23	McD-2.7m
2453536.8320	-191.81	3.41	McD-2.7m
2453537.8593	-227.78	3.53	McD-2.7m
2453563.7695	-203.6	5.06	McD-2.7m
2453630.7031	-133.1	4.42	McD-2.7m
2453654.6640	-45.35	5.97	McD-2.7m
2453689.5234	1.60	4.12	McD-2.7m
2453864.9257	121.91	5.82	McD-2.7m
2453907.8203	185.28	5.99	McD-2.7m
2453927.7812	220.86	5.65	McD-2.7m
2453969.7539	154.81	6.40	McD-2.7m
2454019.5507	21.55	6.47	McD-2.7m
2454020.6406	53.36	6.11	McD-2.7m
2454309.6367	-100.30	3.83	McD-2.7m
2454348.6250	-128.82	3.32	McD-2.7m
2454555.9492	200.35	3.93	McD-2.7m
2454571.9101	119.94	3.73	McD-2.7m
2454604.8593	107.64	8.21	McD-2.7m
2454606.8632	128.94	8.96	McD-2.7m
2454665.7304	104.19	7.08	McD-2.7m
2454965.9492	-95.17	4.63	McD-2.7m

Table 3: The RV Data

Julian Day	RV (m s^{-1})	σ (m s^{-1})	Dataset
2454990.8437	-87.09	4.25	McD-2.7m
2455288.0000	115.67	6.62	McD-2.7m
2455701.8750	74.10	3.26	McD-2.7m
2455759.8007	25.25	3.41	McD-2.7m
2455786.7968	6.87	5.06	McD-2.7m
2455992.0234	-6.51	5.12	McD-2.7m
2456024.8945	90.47	7.15	McD-2.7m
2456053.9687	41.26	4.61	McD-2.7m
2456113.6953	-2.05	6.19	McD-2.7m
2456141.7070	-69.63	3.62	McD-2.7m
2456179.6835	-33.33	6.62	McD-2.7m
2456239.5429	7.63	4.53	McD-2.7m
2456379.8867	43.32	3.54	McD-2.7m
2456401.9726	31	3.20	McD-2.7m
2456430.8828	99.88	4.06	McD-2.7m
2456465.7968	112.98	3.46	McD-2.7m
2456467.7304	110.62	3.91	McD-2.7m
2456498.8867	90.70	4.12	McD-2.7m
2456524.6054	114.32	4.38	McD-2.7m
2456561.5625	-14.10	6.30	McD-2.7m
2456594.6015	24.02	4.54	McD-2.7m
2456755.9882	-195.58	3.67	McD-2.7m
2456861.7343	-147.14	4.65	McD-2.7m
2456885.6093	-119.03	4.67	McD-2.7m
2456938.6562	-94.063	3.71	McD-2.7m
2456973.5312	-2.6401	4.24	McD-2.7m
2457111.9882	127.59	5.00	McD-2.7m
2457251.6250	146.42	3.60	McD-2.7m
2457279.6992	151.27	4.86	McD-2.7m
2457280.5781	145.24	4.62	McD-2.7m
2457437.9687	-0.36	4.38	McD-2.7m
2457465.0156	28.28	4.15	McD-2.7m
2457495.9804	-10.35	3.40	McD-2.7m
2457524.8515	-31.51	4.22	McD-2.7m
2457544.8632	-107.57	4.74	McD-2.7m
2457639.6445	14.3	4.67	McD-2.7m

Table 3: The RV Data

Julian Day	RV (m s^{-1})	σ (m s^{-1})	Dataset
2452776.0898	-79.01	5.62	BOAO
2452777.1054	-139.63	4.45	BOAO
2452778.2460	-125.98	4.16	BOAO
2452779.1093	-119.86	6.75	BOAO
2452780.2148	-138.01	3.27	BOAO
2452781.1367	-173.94	4.94	BOAO
2452948.9335	-109.11	4.77	BOAO
2452949.9375	-89.51	6.68	BOAO
2452975.9257	-133.97	5.08	BOAO
2452977.9023	-120.01	4.42	BOAO
2452980.8867	-117.38	6.78	BOAO
2453044.3593	-22.86	5.09	BOAO
2453045.3281	42.25	3.67	BOAO
2453046.3203	-3.81	4.27	BOAO
2453073.3359	-18.61	5.05	BOAO
2453096.2304	80.22	3.96	BOAO
2453130.3046	86.90	2.09	BOAO
2453131.2265	157.84	3.28	BOAO
2453132.2617	116.42	3.79	BOAO
2453133.0898	69.59	4.52	BOAO
2453299.9687	-15.76	8.02	BOAO
2453302.9531	-51.36	4.87	BOAO
2453395.3437	34.19	4.09	BOAO
2453430.3593	-0.31	4.13	BOAO
2453433.3554	-23.97	3.48	BOAO
2453459.1640	-40.81	5.90	BOAO
2453460.2734	-69.26	4.13	BOAO
2453507.2187	-124.16	4.38	BOAO
2453545.1132	-233.91	6.10	BOAO
2453700.9531	29.04	6.64	BOAO
2453728.8906	62.39	5.70	BOAO
2453778.3398	77.79	4.56	BOAO

Table 3: The RV Data

Julian Day	RV (m s^{-1})	σ (m s^{-1})	Dataset
2453809.3671	210.79	4.45	BOAO
2453818.3203	249.19	4.17	BOAO
2453819.3046	218.99	6.20	BOAO
2453821.2578	209.49	5.80	BOAO
2453867.1757	179.32	3.57	BOAO
2453888.0546	109.29	7.30	BOAO
2453891.1562	112.49	7.40	BOAO
2453896.2148	188.69	6.60	BOAO
2453899.2382	209.79	6.10	BOAO
2453981.0820	152.19	6.40	BOAO
2454017.9570	75.04	4.525	BOAO
2454026.9531	68.59	5.400	BOAO
2454124.3828	-31.81	6.80	BOAO
2454147.3750	-123.56	4.36	BOAO
2454210.2617	-214.61	7.20	BOAO
2454213.3125	-110.21	7.50	BOAO
2454262.2656	-229.11	5.05	BOAO
2454264.2734	-224.91	5.02	BOAO
2454483.4179	39.165	3.01	BOAO
2454506.3750	169.11	3.15	BOAO
2454536.3242	144.01	3.31	BOAO
2454619.0820	117.94	5.55	BOAO
2454643.2539	87.34	5.19	BOAO
2454719.0000	7.99	4.73	BOAO
2454720.0703	13.74	3.95	BOAO
2454735.9843	12.19	4.70	BOAO
2454752.0234	34.19	4.49	BOAO
2454756.0312	49.49	6.40	BOAO
2454847.3906	-99.71	4.27	BOAO
2454931.1484	-128.71	4.34	BOAO
2454971.2460	-191.61	6.70	BOAO
2454995.2109	-69.71	5.90	BOAO
2455130.9492	126.62	3.31	BOAO
2455248.3828	95.29	5.70	BOAO

Table 3: The RV Data

Julian Day	RV (m s^{-1})	σ (m s^{-1})	Dataset
2455321.3164	90.79	5.50	BOAO
2455356.1679	74.19	6.00	BOAO
2455455.9765	127.89	6.0	BOAO
2455671.2773	113.19	6.10	BOAO
2455729.2617	30.49	5.80	BOAO
2455841.9804	6.19	4.06	BOAO
2456024.2500	26.89	7.20	BOAO
2456176.9765	-26.61	4.27	BOAO
2456378.1875	46.19	4.20	BOAO
2456551.9609	24.39	6.00	BOAO
2456616.8945	16.99	6.10	BOAO
2456800.1367	-248.31	6.80	BOAO
2456920.9765	-216.01	7.80	BOAO
2457094.2304	87.59	7.70	BOAO
2457169.2578	92.59	8.20	BOAO
2457300.9296	95.49	5.80	BOAO
2452656.6640	-51.53	5.95	TLS
2452657.6015	-24.90	6.28	TLS
2452713.5937	-102.04	6.93	TLS
2452752.4609	-88.57	5.59	TLS
2452802.3828	-144.46	4.17	TLS
2452804.3671	-180.28	5.91	TLS
2452807.3671	-211.63	4.01	TLS
2452835.3867	-181.19	3.46	TLS
2452836.3750	-285.53	3.25	TLS
2452838.4687	-142.71	3.69	TLS
2452839.4218	-141.16	3.47	TLS
2452840.4375	-158.05	3.53	TLS
2452811.3593	-177.85	2.85	TLS
2452877.3125	-115.81	3.58	TLS
2452878.3203	-182.02	4.03	TLS
2452928.2500	-132.24	3.73	TLS

Table 3: The RV Data

Julian Day	RV (m s^{-1})	σ (m s^{-1})	Dataset
2452929.2500	-104.39	3.65	TLS
2452949.2421	-65.93	3.74	TLS
2453222.3867	87.45	2.56	TLS
2453432.5429	-155.44	3.13	TLS
2453454.6796	-86.94	3.99	TLS
2453477.5625	-5.75	2.76	TLS
2453491.5078	-84.56	6.40	TLS
2453511.4140	-112.12	3.11	TLS
2453528.4179	-150.35	3.79	TLS
2453566.3554	-202.68	1.61	TLS
2453598.3750	-141.15	2.63	TLS
2453599.3359	-167.32	2.86	TLS
2453873.5078	242.19	4.01	TLS
2453877.4296	173.42	2.95	TLS
2453986.4375	127.05	2.66	TLS
2454253.3750	-211.41	4.31	TLS
2454520.5859	165.29	12.95	TLS
2454529.7031	155.51	11.35	TLS
2454530.5078	148.95	15.28	TLS
2454538.6015	162.47	11.78	TLS
2454539.5117	121.29	14.63	TLS
2454614.5742	65.91	11.79	TLS
2454615.5468	100.80	9.50	TLS
2454662.3750	93.39	2.35	TLS
2454663.5781	61.90	2.58	TLS
2454667.5546	22.02	2.48	TLS
2454671.3671	74.42	2.62	TLS
2454694.3906	65.87	2.64	TLS
2454695.4140	62.73	1.94	TLS
2454696.3359	22.82	2.64	TLS
2454759.2343	16.97	2.12	TLS
2454760.2265	-13.25	2.63	TLS

Table 3: The RV Data

Julian Day	RV (m s^{-1})	σ (m s^{-1})	Data Set
2454781.2421	-45.85	3.04	TLS
2454782.3046	-12.66	2.53	TLS
2454783.2304	28.75	2.49	TLS
2454815.7421	-108.13	3.27	TLS
2454840.7500	-145.79	3.66	TLS
2454841.7539	-95.51	3.05	TLS
245484McD-2.7578	-65.23	3.14	TLS
2454843.7539	-148.86	3.30	TLS
2454845.7578	-92.58	3.21	TLS
2454902.6953	-97.77	3.13	TLS
2454904.6601	-146.65	4.28	TLS
2454908.6796	-158.51	3.09	TLS
2454952.3671	-124.95	4.30	TLS
2454954.3281	-123.82	2.97	TLS
2454959.3203	-141.60	3.19	TLS
2454960.5625	-138.76	3.31	TLS
2454999.3906	-46.32	3.02	TLS
2455000.4648	-59.69	4.63	TLS
2455001.4140	-113.96	2.78	TLS
2455002.4140	-113.87	2.97	TLS
2455003.5156	-100.24	2.90	TLS
2455004.3906	-96.63	3.15	TLS
2455035.3750	-91.25	2.79	TLS
2455037.3750	-17.32	2.64	TLS
2455038.3750	-26.16	2.57	TLS
2455039.4648	-48.45	2.13	TLS
2455051.3437	14.03	2.83	TLS
2454267.4453	-30.12	1.89	TLS
2454253.3750	-211.49	4.18	TLS
2454840.7500	-146.43	3.74	TLS
2454841.7539	-95.15	3.04	TLS
245484McD-2.7578	-65.59	3.14	TLS

Table 3: The RV data

Julian Day	RV (m s^{-1})	σ (m s^{-1})	
2454843.7539	-148.69	3.23	TLS
2454845.7578	-92.35	3.18	TLS
2454902.6953	-97.81	3.09	TLS
2454904.6601	-146.57	4.28	TLS
2454908.6796	-158.51	3.09	TLS
2454952.3671	-123.87	4.38	TLS
2454954.3281	-123.96	2.92	TLS
2454959.3203	-140.77	3.16	TLS
2454960.5625	-139.74	3.41	TLS
2454999.3906	-46.12	3.00	TLS
2455000.4648	-59.28	4.65	TLS
2455001.4140	-113.97	2.78	TLS
2455002.4140	-113.87	2.97	TLS
2455003.5156	-100.24	2.90	TLS
2455004.3906	-96.57	3.14	TLS
2455035.3750	-91.79	2.77	TLS
2455037.3750	-16.83	2.65	TLS
2455038.3750	-26.15	2.63	TLS
2455039.4648	-48.32	2.11	TLS
2455051.3437	14.60	2.84	TLS
2455057.3320	-54.30	2.54	TLS
2455155.3046	198.13	2.31	TLS
2455157.3398	106.63	6.52	TLS
2455158.2265	100.18	2.29	TLS
2455161.2265	125.29	2.06	TLS
2455162.2734	104.79	2.36	TLS
2455163.2343	71.02	2.13	TLS
2455168.2500	9.95	2.77	TLS
2455170.2812	139.16	2.71	TLS
2455173.2460	61.14	2.68	TLS
2455175.2500	45.02	2.69	TLS
2455192.1796	40.14	2.99	TLS

Table 3: The RV data

Julian Day	RV (m s^{-1})	σ (m s^{-1})	Data Set
2455193.1992	70.86	2.97	TLS
2455194.2968	69.48	3.31	TLS
2455254.6953	117.42	5.17	TLS
2455258.5781	64.17	4.84	TLS
2455280.4375	69.01	3.13	TLS
2455356.5078	44.13	3.94	TLS
2455450.3476	31.79	3.49	TLS
2455463.3515	29.63	2.41	TLS
2455473.2578	-10.70	2.38	TLS
2455474.2421	38.88	2.47	TLS
2455476.3281	-55.21	1.70	TLS
2455478.3203	50.83	1.80	TLS
2455479.2421	79.10	2.54	TLS
2455480.2460	7.88	2.35	TLS
2455495.2343	59.36	2.50	TLS
2455496.3515	31.56	2.51	TLS
2455498.3515	-9.58	2.56	TLS
2455664.4609	-76.03	3.09	TLS
2455680.4062	48.53	4.90	TLS
2455941.6953	-37.13	6.54	TLS
2456060.4882	24.67	13.26	TLS
2456061.5039	22.32	12.00	TLS
2456103.4531	-42.60	9.56	TLS
2456501.4687	46.14	3.06	TLS

Table 3: The RV data

Parameter	Value
Period [days]	702.47 ± 1.40
T_0 [JD-2440000]	6610.16 ± 38.8
K [m s^{-1}]	148.4 ± 4.1
e	0.08 ± 0.03
ω [deg]	234.26 ± 19.8
$f(m)$ [solar masses]	$(2.35 \pm 0.18) \times 10^{-7}$
$m \sin i$ [$M_{Jupiter}$]	10.7 ± 0.6
a [AU]	

Table 4: Orbital parameters for the hypothetical companion to γ Dra.

Period (d)	K (m s^{-1})	Phase
665.8 ± 3.8	125.73 ± 6.95	0.32 ± 0.03
800.9 ± 10.2	45.52 ± 7.17	0.97 ± 0.02
1854.9 ± 73.9	27.44 ± 8.55	0.30 ± 0.11

Table 5: Frequencies from pre-whitening of the RV data

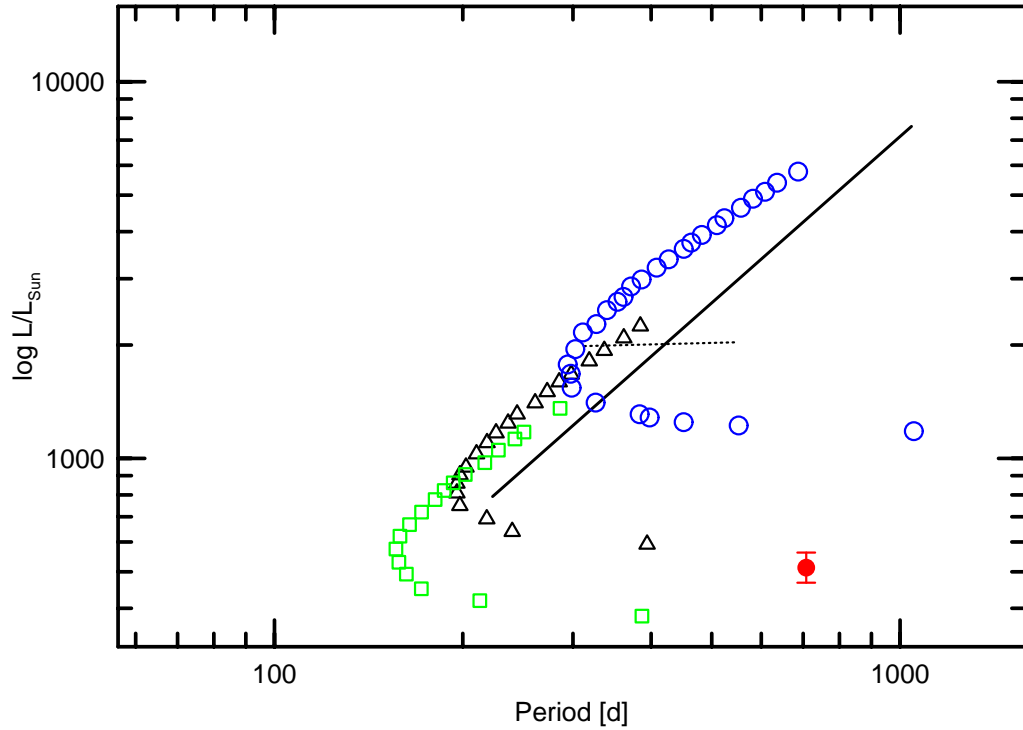


Fig. 9.— Period-Luminosity relations of dipole oscillatory convection modes (circle) taken from Saio et al. (2015). The models shown are representative cases calculated using a mixing length, $\alpha = 1.2$ and for stellar masses of 1.0 (squares), 1.3 (triangles), and 2.0 (circles) M_{\odot} . The diagonal line represents a fit to red giants found in the LMC by Soszynski et al. (2009). The horizontal line dashed line represents the approximate spread of variables in the LMC. The dot marks the location of γ Dra.